Stabilizing Fulde-Ferrell-Larkin-Ovchinnikov superfluidity with long-range interactions in a mixed-dimensional Bose-Fermi system

Jonatan Melkær Midtgaard and Georg M. Bruun
Department of Physics and Astronomy, Aarhus University, DK-8000 Aarhus C, Denmark

(Received 29 May 2018; published 24 July 2018)

We analyze the stability of inhomogeneous superfluid phases in a system consisting of identical fermions confined in two layers that are immersed in a Bose-Einstein condensate (BEC). The fermions in the two layers interact via an induced interaction mediated by the BEC, which gives rise to pairing. We present zero-temperature phase diagrams varying the chemical potential difference between the two layers and the range of the induced interaction, and show that there is a large region where an inhomogeneous superfluid phase is the ground state. This region grows with increasing range of the induced interaction and it can be much larger than for a corresponding system with a short-range interaction. The range of the interaction is controlled by the healing length of the BEC, which makes the present system a powerful tunable platform to stabilize inhomogeneous superfluid phases. We furthermore analyze the melting of the superfluid phases in the layers via phase fluctuations as described by the Berezinskii-Kosterlitz-Thouless mechanism and show that the normal, homogeneous, and inhomogeneous superfluid phases meet in a tricritical point. The superfluid density of the inhomogeneous superfluid phase is reduced by inherent gapless excitations, and we demonstrate that this leads to a significant suppression of the critical temperature as compared to the homogeneous superfluid phase.

DOI: 10.1103/PhysRevA.98.013624

I. INTRODUCTION

The interplay between population imbalance and superfluid pairing has been subjected to intense study ever since Fulde and Ferrell (FF) as well as Larkin and Ovchinnikov (LO) predicted that they can coexist [1,2]. In condensed matter systems, an external magnetic field leads to a population imbalance between the two electron spin projections, which in general is at odds with superconductivity. FFLO however realized that the superconductor can accommodate some population imbalance at the price of giving the Cooper pairs a nonzero center-of-mass (COM) momentum, thereby forming a spatially inhomogeneous but periodic order parameter with no vortices. The fate of superfluid pairing in the presence of population imbalance is a fundamental question relevant for many systems in nature including cold atoms [3–5], superconductors [6], and quark matter [7–9]. Nevertheless, an unambiguous observation of a FFLO phase is still lacking. A major problem for electronic superconductors is that orbital effects due to the magnetic field lead to the formation of vortices and eventually destroy pairing before any FFLO physics can be observed. One strategy to avoid this problem is to explore low-dimensional systems, where orbital effects are suppressed due to the confinement. Indeed, results consistent with a FFLO phase have been reported for quasi-two-dimensional (quasi-2D) organic and heavy fermion superconductors [10–12]. Theoretical studies have furthermore concluded that the FFLO phase is favored in 2D as compared to 3D [13–15].

Quantum degenerate atomic gases are well suited to investigate FFLO physics, because they do not suffer from orbital effects as the atoms are neutral. In addition, it is relatively straightforward to make low-dimensional systems, and signatures of FFLO physics have indeed been observed in a one-dimensional (1D) atomic Fermi gas [16]. There have been a number of investigations of the FFLO phase for 2D atomic gases with a short-range interaction [17–23]. Recently, it was argued that long-range interactions further increase the region of stability of the FFLO phase for a 2D gas of dipolar atoms as compared to a short-range interaction [24,25].

Here, we investigate how to stabilize FFLO superfluidity using a mixed-dimensional system with a tuneable-range interaction. The system consists of fermions confined in two layers immersed in a BEC. The induced interaction between the layers mediated by the BEC gives rise to pairing, and we analyze the stability of the corresponding superfluid phases. We show that the zero-temperature phase diagram as a function of the chemical potential difference in the two layers and the range of the interaction has a large region where an inhomogeneous superfluid phase is the ground state. This region grows with increasing range of the interaction and becomes much wider than for a zero-range interaction. The interaction range can be tuned by varying the healing length of the BEC. We furthermore investigate the melting of the 2D superfluid phases via the Berezinskii-Kosterlitz-Thouless mechanism. The normal phase and the homogeneous and inhomogeneous superfluid phases are shown to meet in a tricritical point in the phase diagram, which determines the maximum critical temperature of the inhomogeneous superfluid. This maximum temperature is, however, significantly suppressed compared to the homogeneous superfluid phase, due to inherent gapless excitations, which decrease the superfluid density.

II. THE BILAYER SYSTEM

We consider the system illustrated in Fig. 1. Two layers contain fermions of a single species with mass m, and they are immersed in a 3D weakly interacting BEC consisting of bosons

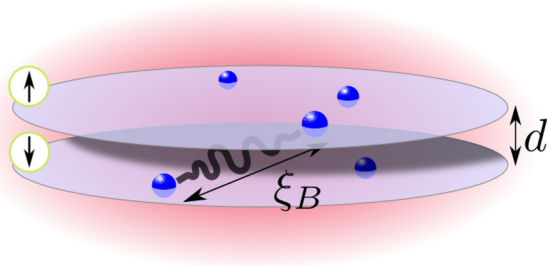

FIG. 1. A sketch of the considered system. The fermions (blue) are confined in two layers immersed in a three-dimensional BEC (red), with a layer distance d. The BEC mediates an interaction between fermions in the two different layers of the Yukawa form, with a range determined by the BEC healing length ξ_B.

with mass m_B and density n_B. The distance between the layers is d and the surface density of fermions in each layer is n_σ with $\sigma = \uparrow,\downarrow$ denoting the two layers. When used in equations, they are taken to mean $\uparrow = +1$, $\downarrow = -1$, respectively. Occasionally we will also use the notation $\bar{\sigma}$ to mean the opposite layer from σ. The boson-fermion interaction is short range and characterized by the strength $g = 2\pi a_{\rm eff}/\sqrt{m_r m_B}$, with $m_r = mm_B/(m+m_B)$ the reduced mass and $a_{\rm eff}$ the effective 2D-3D scattering length [26]. Throughout, this interaction strength is taken to be weak in the sense $k_{F\sigma}a_{\rm eff} \ll 1$, where $k_{F\sigma} = \sqrt{4\pi n_\sigma}$ is the Fermi momentum of layer σ.

We treat the BEC using zero-temperature Bogoliubov theory. This is a good approximation since the critical temperature of the superfluid phases of the fermions is much smaller than the critical temperature of the BEC. The bosonic degrees of freedom can then be integrated out, which yields an effective interaction between the fermions. In the static limit, this interaction is on the Yukawa form, and we end up with an effective Hamiltonian for the fermions in the two layers of the form [27–29]

$$H = H_{\rm kin} + H_{\rm int} = \sum_{\mathbf{k},\sigma} \xi_{\mathbf{k}\sigma} c^\dagger_{\mathbf{k}\sigma} c_{\mathbf{k}\sigma} + \frac{1}{2\mathcal{V}} \sum_{\sigma,\sigma'} \sum_{\mathbf{k},\mathbf{k}',\mathbf{q}} V_{\sigma\sigma'}(\mathbf{q}) c^\dagger_{\mathbf{k}+\mathbf{q}\sigma} c^\dagger_{\mathbf{k}'-\mathbf{q}\sigma'} c_{\mathbf{k}'\sigma'} c_{\mathbf{k}\sigma}. \quad (1)$$

Here, $c^\dagger_{\mathbf{k}\sigma}$ creates a fermion in layer σ with 2D momentum $\mathbf{k} = (k_x, k_y)$, the dispersion in each layer is $\xi_{\mathbf{k}\sigma} = k^2/2m - \mu_\sigma$ with μ_σ the chemical potentials, and $\mathcal{V}$ is the system volume. We define the average chemical potential $\mu = (\mu_\uparrow + \mu_\downarrow)/2$ and the "magnetic field" $h = (\mu_\downarrow - \mu_\uparrow)/2$, so that we can write $\xi_{\mathbf{k}\sigma} = k^2/2m - \mu + \sigma h$. The Yukawa interaction is

$$V_{\sigma\sigma'}(\mathbf{q}) = -\frac{2g^2 n_B m_B}{\sqrt{q^2 + 2/\xi_B^2}} e^{-\sqrt{q^2+2/\xi_B^2}|\sigma-\sigma'|d/2}, \quad (2)$$

where $\xi_B = 1/\sqrt{8\pi n_B a_B}$ is the healing length of the BEC with a_B the boson-boson scattering length. The healing length determines the range of the induced interaction, as can be seen by Fourier transforming Eq. (2) to real space, giving $V(r) = -g^2 n_B m_B \pi^{-1} \exp(-\sqrt{2}r/\xi_B)/r$ with r the 3D distance between the fermions. It follows that the range of the interaction can be tuned by varying the density n_B or the scattering length a_B of the surrounding BEC, which turns out to be a key property for the following. We note that retardation effects can be neglected when the speed of sound in the BEC is much larger than the Fermi velocity in the two planes [28].

III. PAIRING AND GREEN'S FUNCTIONS

The attractive interaction given by Eq. (2) can lead to Cooper pairing within each layer (intralayer pairing), and between the two layers (interlayer pairing). We recently analyzed the competition between intra- and interlayer pairing for the case of equal density in each layer, i.e., for $n_\uparrow = n_\downarrow$ [29]. For a layer distance d large compared to the range ξ_B of the interaction, we found that the ground state is characterized by intralayer p-wave pairing, whereas s-wave interlayer pairing is stable for smaller d/ξ_B. In addition, we identified a crossover phase for intermediate d/ξ_B where both types of pairing coexist.

In this paper, we focus on interlayer s-wave pairing corresponding to $d/\xi_B \lesssim 1$. We shall investigate the case of a nonzero field h giving rise to a population difference between the two layers, and the possibility of FFLO interlayer pairing with nonzero COM momentum. Such interlayer pairing with COM momentum $\mathbf{Q}$ is characterized by the anomalous averages $\langle c_{\mathbf{Q}/2+\mathbf{k}\sigma} c_{\mathbf{Q}/2-\mathbf{k},\bar{\sigma}}\rangle$, which leads us to define the corresponding pairing field

$$\Delta_{\sigma\bar{\sigma}}(\mathbf{k},\mathbf{Q}) = \frac{1}{\mathcal{V}} \sum_{\mathbf{k}'} V(\mathbf{k}-\mathbf{k}') \langle c_{\mathbf{Q}/2+\mathbf{k}'\sigma} c_{\mathbf{Q}/2-\mathbf{k}',\bar{\sigma}}\rangle. \quad (3)$$

We have dropped the subscripts on the induced interaction $V(\mathbf{q})$, as here and in the following it refers to the interlayer interaction only, i.e., $V(\mathbf{q}) \equiv V_{\sigma\bar{\sigma}}(\mathbf{q})$. The pairing field obeys the Fermi antisymmetry $\Delta_{\sigma\bar{\sigma}}(\mathbf{k},\mathbf{Q}) = -\Delta_{\bar{\sigma}\sigma}(-\mathbf{k},\mathbf{Q})$. In real space, it is of the form

$$\Delta_{\sigma\bar{\sigma}}(\mathbf{r}_1,\mathbf{r}_2) = V(\mathbf{r}_1-\mathbf{r}_2)\langle\psi_\sigma(\mathbf{r}_1)\psi_{\bar{\sigma}}(\mathbf{r}_2)\rangle = \frac{1}{\mathcal{V}} \sum_{\mathbf{Q},\mathbf{k}} \Delta_{\sigma\bar{\sigma}}(\mathbf{k},\mathbf{Q}) e^{i\mathbf{Q}\cdot\mathbf{R}} e^{i\mathbf{k}\cdot\mathbf{r}}, \quad (4)$$

where $\mathbf{R} = (\mathbf{r}_1+\mathbf{r}_2)/2$ and $\mathbf{r} = \mathbf{r}_1 - \mathbf{r}_2$ are the COM and relative coordinates respectively, and $\psi_\sigma(\mathbf{r}) = \sum_{\mathbf{k}} c_{\mathbf{k}\sigma} \exp(\mathbf{k}\cdot\mathbf{r})$ is the field operator for particles in layer σ. We note that the pairing field is not translationally symmetric in the FFLO phase, i.e., $\Delta_{\sigma\bar{\sigma}}(\mathbf{r}_1,\mathbf{r}_2) \neq \Delta_{\sigma\bar{\sigma}}(\mathbf{r}_1-\mathbf{r}_2)$. The interaction becomes in the mean-field BCS approximation

$$H^{\rm MF}_{\rm int} = \sum_{\mathbf{Q},\mathbf{k}} \Delta_{\uparrow\downarrow}(\mathbf{k},\mathbf{Q}) c^\dagger_{\mathbf{Q}/2-\mathbf{k}\downarrow} c^\dagger_{\mathbf{Q}/2+\mathbf{k}\uparrow} + \text{H.c.}, \quad (5)$$

where we include only the pairing channel as we focus on the superfluid instability. The Hartree-Fock terms will in general lead to small effects in the weak coupling regime, which mostly can be accounted for by a renormalization of the chemical potentials μ_σ.

All results presented here can be obtained by a direct diagonalization of the mean-field BCS Hamiltonian $H^{\rm MF} = H_0 + H^{\rm MF}_{\rm int}$ using a standard Bogoliubov transformation. We, however, use Green's functions to analyze the FFLO states, since this formalism naturally allows us to go beyond mean-field theory to include effects such as retardation, if needed in the future. The normal and anomalous Green's functions for

the superfluid phases are defined in the standard way as

$$\begin{aligned} G_\sigma(\mathbf{k},\mathbf{k}',\tau) &= -\langle T_\tau c_{\mathbf{k}\sigma}(\tau) c^\dagger_{\mathbf{k}'\sigma}(0)\rangle, \\ F_\sigma(\mathbf{k},\mathbf{k}',\tau) &= -\langle T_\tau c_{\mathbf{k}\sigma}(\tau) c_{-\mathbf{k}',\bar\sigma}(0)\rangle, \\ F^\dagger_\sigma(\mathbf{k},\mathbf{k}',\tau) &= -\langle T_\tau c^\dagger_{-\mathbf{k},\sigma}(\tau) c^\dagger_{\mathbf{k}'\bar\sigma}(0)\rangle, \end{aligned} \tag{6}$$

where T_τ denotes imaginary-time ordering. Using $H^{\rm MF} = H_{\rm kin} + H^{\rm MF}_{\rm int}$, the Gor'kov equations for these Green's functions are straightforwardly derived. They read

$$\begin{aligned} &(i\omega_n - \xi_{\mathbf{k}\sigma}) G_\sigma(\mathbf{k},\mathbf{k}',\omega_n) \\ &\quad = \delta_{\mathbf{k},\mathbf{k}'} - \sum_{\mathbf{Q}} \Delta_{\sigma\bar\sigma}(\mathbf{k}-\mathbf{Q}/2,\mathbf{Q}) F^\dagger_{\bar\sigma}(\mathbf{k}-\mathbf{Q},\mathbf{k}',i\omega_n), \end{aligned} \tag{7}$$

$$\begin{aligned} &(i\omega_n - \xi_{\mathbf{k}\sigma}) F_\sigma(\mathbf{k},\mathbf{k}',\omega_n) \\ &\quad = \sum_{\mathbf{Q}} \Delta_{\sigma\bar\sigma}(\mathbf{k}-\mathbf{Q}/2,\mathbf{Q}) G_\sigma(-\mathbf{k}',-\mathbf{k}+\mathbf{Q},-i\omega_n), \end{aligned} \tag{8}$$

$$\begin{aligned} &(i\omega_n + \xi_{-\mathbf{k},\sigma}) F^\dagger_\sigma(\mathbf{k},\mathbf{k}',\omega_n) \\ &\quad = \sum_{\mathbf{Q}} \Delta^*_{\sigma\bar\sigma}(-\mathbf{k}-\mathbf{Q}/2,\mathbf{Q}) G_{\bar\sigma}(\mathbf{k}+\mathbf{Q},\mathbf{k}',i\omega_n), \end{aligned} \tag{9}$$

where we have Fourier transformed to Matsubara frequency space with $\omega_n = (2n+1)\pi T$. The self-consistent gap equation is then from (3) and (6)

$$\begin{aligned} \Delta_{\sigma\bar\sigma}(\mathbf{k},\mathbf{Q}) = -\frac{T}{\mathcal{V}} \sum_{\mathbf{k}',n} V(\mathbf{k}-\mathbf{k}') \\ \times F_\sigma(\mathbf{Q}/2+\mathbf{k}'/2, \mathbf{k}'-\mathbf{Q}/2, i\omega_n) e^{-i\omega_n 0_+}. \end{aligned} \tag{10}$$

IV. FULDE-FERREL SUPERCONDUCTIVITY

The $\mathbf{Q}$ values for which $\Delta_{\sigma\bar\sigma}(\mathbf{k},\mathbf{Q})$ is nonzero determine the structure of the order parameter in the superfluid phase. It has been shown that $\Delta_{\sigma\bar\sigma}(\mathbf{r}_1,\mathbf{r}_2)$ can form very complicated 2D structures corresponding to $\Delta_{\sigma\bar\sigma}(\mathbf{k},\mathbf{Q}) \neq 0$ for many $\mathbf{Q}$'s in Eq. (4) [30,31]. However, the FFLO phase exhibits a second-order transition to the normal phase in 2D at an upper critical field h_{c2} [13,14], and at this transition it is sufficient to consider the case of $\Delta_{\sigma\bar\sigma}(\mathbf{k},\mathbf{Q}) \neq 0$ only for a single $\mathbf{Q}$ vector. The reason is that any linear combination of the $\Delta_{\sigma\bar\sigma}(\mathbf{k},\mathbf{Q})$'s, which are unstable towards pairing, is degenerate at h_{c2}, since it is only the nonlinear part of the gap equation that determines the optimal combination that minimizes the energy.

In the following, we therefore consider the case $\Delta_{\sigma\bar\sigma}(\mathbf{k},\mathbf{Q}) \neq 0$ only for a single $\mathbf{Q}$. This will give the correct upper critical field h_{c2} for the second-order transition between the FFLO and the normal phase. We also expect that it will give a fairly precise value for the lower critical field h_{c1} determining the first-order transition between the FFLO and the superfluid phase, since the energy difference between the FFLO phases with various spatial structures is small [30,31]. Our scheme recovers the usual homogenous BCS pairing for $\mathbf{Q} = 0$, and it corresponds to a plane wave Fulde-Ferrel (FF) type of pairing when $\mathbf{Q} \neq 0$, as can be seen from Eq. (4). Since we only have one $\mathbf{Q}$ vector, we can simplify the notation for the gap as $\Delta_{\sigma\bar\sigma}(\mathbf{k},\mathbf{Q}) \to \Delta_{\sigma\bar\sigma}(\mathbf{k})$. The Gor'kov equations (7)–(9) are then easily solved, giving

$$\begin{aligned} G_\sigma(\mathbf{k},\mathbf{k}' i\omega_n) &= \delta_{\mathbf{k},\mathbf{k}'} \left(i\omega_n - \xi_{\mathbf{k},\sigma} - \frac{|\Delta_{\sigma\bar\sigma}(\mathbf{k}-\mathbf{Q}/2)|^2}{i\omega_n + \xi_{-\mathbf{k}+\mathbf{Q},\bar\sigma}} \right)^{-1}, \\ F_\sigma(\mathbf{k},\mathbf{k}',i\omega_n) &= \frac{\Delta_{\sigma\bar\sigma}(\mathbf{k}-\mathbf{Q}/2)}{i\omega_n - \xi_{\mathbf{k}\sigma}} G_\sigma(\mathbf{k},\mathbf{k}' i\omega_n). \end{aligned} \tag{11}$$

Using Eq. (11) in Eq. (10), we obtain the gap equation

$$\Delta(\mathbf{k}) = -\int d^2\check{k}' V(\mathbf{k}-\mathbf{k}') \frac{\Delta(\mathbf{k}')}{2E_{\mathbf{k}'}} [1 - f^+_{\mathbf{k}'} - f^-_{\mathbf{k}'}], \tag{12}$$

where $E^\pm_{\mathbf{k}'} = E_{\mathbf{k}'} \pm (h + \frac{\mathbf{k}'\cdot\mathbf{Q}}{2m})$, with $E_{\mathbf{k}'} = [(\mathbf{k}'^2/2m + \mathbf{Q}^2/8m - \mu)^2 + |\Delta(\mathbf{k}')|^2]^{1/2}$, and the Fermi distribution function is $f^\pm_{\mathbf{k}} = [\exp(\beta E^\pm_{\mathbf{k}}) + 1]^{-1}$. In Eq. (12) and the rest of this paper, we have further simplified the notation by defining $\Delta_{\uparrow\downarrow}(\mathbf{k}) \to \Delta(\mathbf{k})$ and $d^2\check{k}' = d^2k'/(2\pi)^2$. We solve Eq. (12) along with the number equation

$$N = \sum_{\mathbf{k}} \left[1 - \frac{\xi_{\mathbf{k}} + q^2/8m}{E_{\mathbf{k}}} \left(1 - f^+_{\mathbf{k}} - f^-_{\mathbf{k}}\right) \right]. \tag{13}$$

Note that in order to compare with previous results in the literature, we keep the *total* number of particles, $N = N_\uparrow + N_\downarrow$, fixed, and not the number of particles in each plane. To solve the gap equation (12), we perform a partial wave expansion of the induced interaction $V(\mathbf{k}) = \sum_n V_n(k) \exp(in\phi_{\mathbf{k}})$, where $\phi_{\mathbf{k}}$ is the azimuthal angle of $\mathbf{k}$. In the numerics, we keep the two leading terms, $n = 0, 1$ corresponding to s-wave singlet and p-wave triplet pairing respectively. When solving the above equations, we find three different phases: The homogeneous BCS phase with $\mathbf{Q} = 0$, the FF state with $\mathbf{Q} \neq 0$, and the normal phase with no superfluid pairing. To determine which of these phases is the ground state, we compare their energy E. We have from mean-field theory

$$\begin{aligned} E - \mu_\uparrow N_\uparrow - \mu_\downarrow N_\downarrow = \sum_{\mathbf{k}} \xi_{\mathbf{k}} - \sum_{E^-_{\mathbf{k}}>0} E^-_{\mathbf{k}} + \sum_{E^+_{\mathbf{k}}<0} E^+_{\mathbf{k}} \\ + \sum_{\mathbf{k}} \frac{|\Delta(\mathbf{k})|^2}{2E_{\mathbf{k}}} (1 - f^+_{\mathbf{k}} - f^-_{\mathbf{k}}). \end{aligned} \tag{14}$$

V. RESULTS FOR ZERO TEMPERATURE

We now solve the Gor'kov equations for $T = 0$, varying the interaction range and density imbalance through the healing length ξ_B and the field $h = (\mu_\uparrow - \mu_\downarrow)/2$, respectively. The resulting phase diagrams are shown in Figs. 2 and 3 for two different values of the layer distance, $k_F d = 1$ and $k_F d = 0$. The Fermi momentum is defined as $k_F = \sqrt{2\pi(n_\uparrow + n_\downarrow)}$. We set the effective scattering length to $k_F a_{\rm eff} = 0.05$. This small value ensures that we stay in the valid range of mean-field theory for all parameter sets shown in the figures. As is standard in the literature, we measure the field h in units of $\Delta_0 = \Delta(k_F, \mathbf{0})$, which is the pairing field at the Fermi surface for $h = 0$, that is, with no density imbalance.

Consider first the case of the layer distance $k_F d = 1$. Figure 2 clearly shows that there is a large region in the phase diagram, where the FF phase is stable. We find that the phase transition between the BCS and the FF phase is first order at the lower critical field h_{c_1}, whereas it is second order for the transition between the FF phase and the normal phase at the

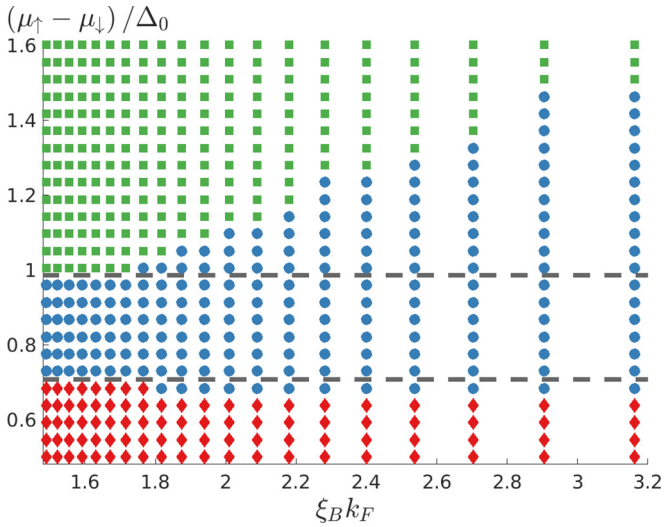

FIG. 2. The $T = 0$ phase diagram of the bilayer fermions for $k_F d = 1$ and $k_F a_{\text{eff}} = 0.05$, as a function of the interaction range ξ_B and the field h. The (red) diamonds, (blue) circles, and (green) squares indicate the BCS, FF, and normal phase, respectively. The horizontal dashed lines give the upper and lower critical fields for the FF phase for a short-range interaction [13,14].

upper critical field h_{c_2}. This is in agreement with the results for a short-range interaction [13,14]. Moreover, the range of values of h for which the FF phase is the ground state increases with the interaction range ξ_B. This shows that a long-range interaction stabilizes the FF phase. The reason is that the relative strength of the p-wave component compared to the s-wave component of the interaction increases with increasing range, which favors FF pairing. To illustrate this important point further, we plot as horizontal lines in Fig. 2 the critical fields for a short-range interaction [1,24], $h_{c_1} \approx \Delta_0/\sqrt{2} \approx 0.7\Delta_0$ and $h_{c_2} = \Delta_0$. While the FF region approaches that of

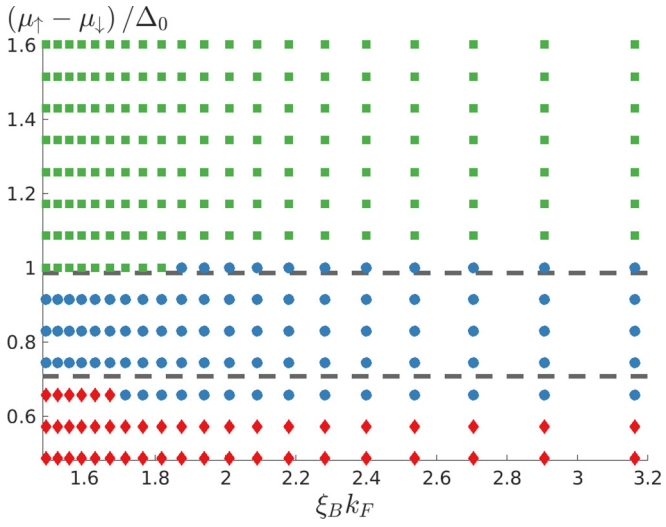

FIG. 3. The $T = 0$ phase diagram of the bilayer fermions as a function of the interaction range ξ_B and the field h for zero layer distance and boson-fermion interaction strength $k_F a_{\text{eff}} = 0.05$. The symbols and lines mean the same as in Fig. 2.

a short-range interaction for decreasing $k_F d$, it becomes much larger with increasing range $k_F \xi_B$.

Consider next the case of zero layer distance $d = 0$ shown in Fig. 3. While a large $k_F \xi_B$ still stabilizes the FF phase, the effect here is much less pronounced as compared to the case $k_F d = 1$. Increasing ξ_B leads to a smaller increase in the range of values of h for which the FF phase is the ground state than for $k_F d = 1$. The reason is that the short-range $1/r$ divergence of the Yukawa interaction between the fermions in the two layers given by Eq. (2) is cut off at $1/d$ for a finite layer distance d. A non-zero value of d makes the p-wave part of the interaction stronger compared to the s-wave part. As a result, the FF phase where there is pairing in both the s- and p-wave channels is favored compared to the pure s-wave BCS state for a nonzero layer distance. Note that the reason the superfluid region (BCS and FF) seems larger for $k_F d = 1$ compared to $d = 0$ even though the strength of the interaction obviously is smaller for a nonzero layer distance, is that we measure h in units of Δ_0, which is also smaller. Had we used the unit ϵ_F instead for instance, the superfluid region of the $d = 0$ phase would be larger.

VI. BEREZINSKII-KOSTERLITZ-THOULESS MELTING

Since the fermions are confined in 2D layers, phase fluctuations of the order parameter are significant and will eventually melt the superfluid through the Berezinskii-Kosterlitz-Thouless (BKT) mechanism at a critical temperature T_{BKT}. To describe this, we first calculate the superfluid stiffness, or equivalently the superfluid density, by imposing a linear phase twist on the order parameter and calculating the corresponding energy cost to second order in the twist. For a given vector $\mathbf{Q}$, the real space pairing becomes, using Eq. (4),

$$\Delta(\mathbf{R}, \mathbf{R}) = \Delta \cdot e^{i(\mathbf{Q}+\delta\mathbf{q})\cdot\mathbf{R}}, \tag{15}$$

where $\Delta = \sum_{\mathbf{k}} \Delta(\mathbf{k})/\mathcal{V}$ and $\delta\mathbf{q} \cdot \mathbf{R} = \delta\theta(\mathbf{R})$ is the imposed spatially linear phase twist. From Eq. (15), it is clear that the direction of the phase twist relative to the COM of the Cooper pairs is important: When $\delta\mathbf{q}$ is parallel to $\mathbf{Q}$, the phase twist corresponds to adding/removing COM momentum to the Cooper pairs which compresses/expands the wavelength of the plane wave pairing field $\Delta(\mathbf{R}, \mathbf{R})$; when $\delta\mathbf{q}$ is perpendicular to $\mathbf{Q}$, the phase twist corresponds to a small rotation of the COM momentum to the Cooper pairs which rotates the plane wave pairing field. These two effects are illustrated in Fig. 4(a).

The phase twist $\delta\theta(\mathbf{R})$ gives a free energy cost δF of the form

$$\begin{aligned}\delta F &= \frac{1}{2}\int d^2\mathbf{r}[J_\parallel(\partial_\parallel\delta\theta)^2 + J_\perp(\partial_\perp\delta\theta)^2] \\ &= \frac{J}{2}\int d^2\mathbf{r}(\nabla\delta\theta)^2,\end{aligned} \tag{16}$$

where $\partial_\parallel$ and $\partial_\perp$ are spatial derivatives parallel or perpendicular to the COM momentum of the Cooper pairs, corresponding to $\delta\mathbf{q} \parallel \mathbf{Q}$ and $\delta\mathbf{q} \perp \mathbf{Q}$ respectively. The associated superfluid stiffness constants are $J_\parallel$ and $J_\perp$. In the second line of Eq. (16), we have rescaled the spatial coordinate perpendicular to $\mathbf{Q}$ by the factor $\sqrt{J_\parallel/J_\perp}$ to obtain an isotropic XY model with the effective stiffness constant $J = \sqrt{J_\parallel J_\perp}$ [32]. Alternatively, defining the superfluid densities parallel and perpendicular to

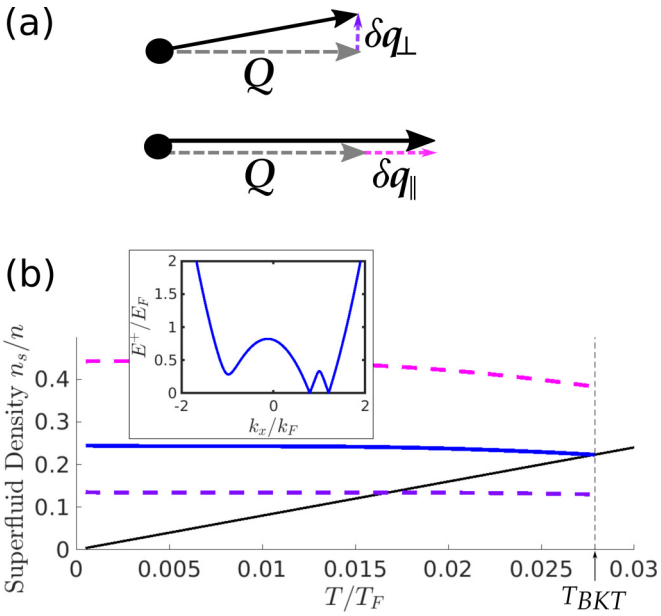

FIG. 4. (a) The two kinds of phase fluctuations with $\delta\mathbf{q}$ perpendicular and parallel to the COM momentum $\mathbf{Q}$ of the Cooper pairs give rise to a rotation and a compression/expansion of the plane wave pairing field respectively. (b) The corresponding superfluid densities $n_{s\parallel}$ (top dashed magenta line) and $n_{s\perp}$ (bottom dashed purple line). The solid blue line is to the effective superfluid density $n_s = \sqrt{n_{s\parallel} n_{s\perp}}$. The critical temperature T_{BKT} is reached when n_s crosses the thin solid black line as indicated by the vertical dashed line. The inset shows one branch of the quasiparticle spectrum along $k_y = 0$ with the COM momentum $\mathbf{Q}$ along the x axis for $T = 0$. The gapless excitations leading to the reduction in the superfluid density are clearly visible.

$\mathbf{Q}$ as $n_{s\perp} = 4mJ_\perp$ and $n_{s\parallel} = 4mJ_\parallel$, we can write the free energy cost as

$$\delta F = m \int d^2\mathbf{r}\left[n_{s\parallel} v_{s\parallel}^2 + n_{s\perp} v_{s\perp}^2\right]/2. \tag{17}$$

Here $v_{s\parallel} = \partial_\parallel \delta\theta/2m$ is the superfluid velocity parallel to $\mathbf{Q}$ and likewise for $v_{s\perp}$. One way to calculate the energy shift due to the phase twist is by considering a corresponding gauge transformed lattice Hamiltonian [33]:

$$H^{\mathrm{MF}}_{\mathrm{latt.}}(\theta) = \exp\left(-i\frac{\delta\theta}{2}\sum_l x_{||,l}/a\right) \times H^{\mathrm{MF}}_{\mathrm{latt.}} \exp\left(-i\frac{\delta\theta}{2}\sum_l x_{||,l}/a\right),$$

where a is the lattice constant and $x_{||,l}$ is the position along the axis parallel to $\mathbf{Q}$ of the lth particle. This can then be expanded to second order and the continuum limit $a \to 0$ taken while keeping the total density constant. This yields

$$n_{s\parallel} = n - \frac{\beta}{m}\int d^2\check{k}[f^+_{\mathbf{k}}(1 - f^+_{\mathbf{k}}) + f^-_{\mathbf{k}}(1 - f^-_{\mathbf{k}})]k^2_\parallel \tag{18}$$

for the superfluid density along $\mathbf{Q}$, where $k_\parallel = \mathbf{k}\cdot\mathbf{Q}/Q$. Here, n is the total surface density of fermions coming from the two layers. An equivalent formula holds for $n_{s\perp}$. Note that the continuum result above can also be obtained directly without considering a lattice system first. Equation (18) is the 2D version of the usual expression for the superfluid density allowing for the effects of the spatial anisotropy of the FF state [34,35]. We can now determine the critical temperature of the superfluid using the BKT condition

$$T_{\mathrm{BKT}} = \frac{\pi}{2}J = \frac{\pi}{8m}n_s, \tag{19}$$

where we have defined the effective superfluid density as $n_s = \sqrt{n_{s\parallel} n_{s\perp}}$.

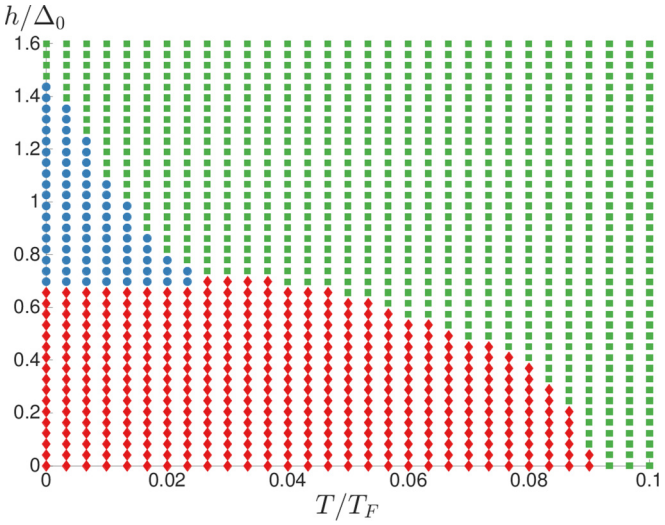

FIG. 5. The phase diagram as a function of temperature T and field h for layer distance $k_F d = 1$, boson-fermion interaction strength $k_F a_{\mathrm{eff}} = 0.05$, and range $k_F \xi_B = 3$. The symbols mean the same as in Figs. 2 and 3.

In Fig. 4(b), we plot the superfluid densities as a function of T for layer distance $k_F d = 1$ and boson-fermion interaction strength $k_F a_{\mathrm{eff}} = 0.05$. We see that $n_{s\parallel} > n_{s\perp}$, reflecting that the energy cost related to compressing/expanding the COM momentum is higher than that related to rotating it as expected. Note that both superfluid densities are smaller than the total density n even for $T \to 0$. This is due to the inherent presence of gapless quasiparticle states in the FF phase. These gapless excitations, which are shown in the inset of Fig. 4(b), reduce the superfluid density. We also plot the effective superfluid density $n_s = \sqrt{n_{s\parallel} n_{s\perp}}$ as well as the line $8mT/\pi$. It follows from Eq. (19) that the superfluid phase melts when n_s crosses this line.

Having set up the theory for BKT melting, we can now analyze the BCS and FF phases at nonzero temperatures. In Fig. 5, we present an example of a phase diagram for $k_F d = 1$ and $k_F a_{\mathrm{eff}} = 0.05$. We see that the critical temperature of the FF phase increases with decreasing field h. The highest critical temperature is obtained just above the lowest critical field h_{c_1}, where the FF, BCS, and normal phase meet in a *tricritical point* at $h_{c_1} \approx 0.7\Delta_0$ and $T \approx 0.025T_F$. This critical temperature is well below the theoretical maximum of $T_F/8$ obtained by setting $n_s = n$ in Eq. (19). The reason is that the gapless excitations in the FF phase decrease the superfluid density below n, as we discussed above in connection with Fig. 4. Indeed, we note that the values of the two components of the superfluid density in Fig. 4 at $T = T_c$ are almost unchanged

from their values at $T \to 0$. This is a general result: While the flexibility of the bilayer system allows us to optimize the induced interaction to favor FF pairing, the gapless nature of this state prevents us from reaching critical temperatures close to $T_F/8$.

The critical temperature of the BCS phase is much higher, as can be seen from Fig. 5. Due to its fully gapped spectrum, T_{BKT} can in fact relatively easily be tuned to be close to maximum $T_F/8$ by varying the layer distance d and the interaction range ξ_B, even while keeping the boson-fermion interaction strength a_{eff} weak.

VII. CONCLUSION

We analyzed a mixed-dimensional system consisting of two layers of identical fermions immersed in a BEC. This system was shown to support superfluid pairing due to an attractive induced interaction between the two layers mediated by the BEC. When the densities of the two layers are different, the resulting superfluid phase is inhomogeneous. Using a plane wave FF ansatz to describe this phase, we demonstrated that it is stabilized by the nonzero range of the induced interaction. Importantly, the FF phase can occupy much larger regions of the phase diagram as compared to the case of a short-range interaction. The range of the induced interaction can be tuned by varying the BEC healing length, which makes the present system promising for realizing FFLO physics experimentally. We furthermore analyzed the melting of the superfluid phases due to phase fluctuations using BKT theory, and demonstrated that the normal, homogenous, and inhomogeneous superfluid phases meet in a tricritical point in the phase diagram. The superfluid density of the FF phase was shown to be suppressed by intrinsic gapless excitations, and this leads to a significant reduction in the critical temperature compared to the homogeneous superfluid, which can be tuned to have a critical temperature close to the maximum $T_F/8$.

ACKNOWLEDGMENT

We wish to acknowledge the support of the Danish Council of Independent Research - Natural Sciences via Grant No. DFF-4002-00336.

[1] P. Fulde and R. A. Ferrell, Phys. Rev. **135**, A550 (1964).
[2] A. I. Larkin and Yu. N. Ovchinnikov, Zh. Eksp. Teor. Fiz. **47**, 1136 (1964) [Sov. Phys. JETP **20**, 762 (1965)].
[3] F. Chevy and C. Mora, Rep. Prog. Phys. **73**, 112401 (2010).
[4] L. Radzihovsky and D. E. Sheehy, Rep. Prog. Phys. **73**, 076501 (2010).
[5] J. J. Kinnunen, J. E. Baarsma, J.-P. Martikainen, and P. Törmä, Rep. Prog. Phys. **81**, 046401 (2018).
[6] Y. Matsuda and H. Shimahara, J. Phys. Soc. Jpn. **76**, 051005 (2007).
[7] R. Casalbuoni and G. Nardulli, Rev. Mod. Phys. **76**, 263 (2004).
[8] M. G. Alford, A. Schmitt, K. Rajagopal, and T. Schäfer, Rev. Mod. Phys. **80**, 1455 (2008).
[9] R. Anglani, R. Casalbuoni, M. Ciminale, N. Ippolito, R. Gatto, M. Mannarelli, and M. Ruggieri, Rev. Mod. Phys. **86**, 509 (2014).
[10] R. Beyer and J. Wosnitza, Low Temp. Phys. **39**, 225 (2013).
[11] H. Mayaffre, S. Krämer, M. Horvatić, C. Berthier, K. Miyagawa, K. Kanoda, and V. F. Mitrović, Nat. Phys. **10**, 928 (2014).
[12] A. Bianchi, R. Movshovich, C. Capan, P. G. Pagliuso, and J. L. Sarrao, Phys. Rev. Lett. **91**, 187004 (2003).
[13] H. Shimahara, Phys. Rev. B **50**, 12760 (1994).
[14] H. Burkhardt and D. Rainer, Ann. Phys. (NY) **506**, 181 (1994).
[15] P. Pieri, D. Neilson, and G. C. Strinati, Phys. Rev. B **75**, 113301 (2007).
[16] Y.-a. Liao, A. S. C. Rittner, T. Paprotta, W. Li, G. B. Partridge, R. G. Hulet, S. K. Baur, and E. J. Mueller, Nature (London) **467**, 567 (2010).
[17] J. Gukelberger, S. Lienert, E. Kozik, L. Pollet, and M. Troyer, Phys. Rev. B **94**, 075157 (2016).
[18] J. E. Baarsma and P. Törmä, J. Mod. Opt. **63**, 1795 (2016).
[19] G. J. Conduit, P. H. Conlon, and B. D. Simons, Phys. Rev. A **77**, 053617 (2008).
[20] L. Radzihovsky and A. Vishwanath, Phys. Rev. Lett. **103**, 010404 (2009).
[21] M. J. Wolak, B. Grémaud, R. T. Scalettar, and G. G. Batrouni, Phys. Rev. A **86**, 023630 (2012).
[22] S. Yin, J.-P. Martikainen, and P. Törmä, Phys. Rev. B **89**, 014507 (2014).
[23] D. E. Sheehy, Phys. Rev. A **92**, 053631 (2015).
[24] H. Lee, S. I. Matveenko, D.-W. Wang, and G. V. Shlyapnikov, Phys. Rev. A **96**, 061602 (2017).
[25] A. Mazloom and S. H. Abedinpour, Phys. Rev. B **96**, 064513 (2017).
[26] Y. Nishida and S. Tan, Phys. Rev. Lett. **101**, 170401 (2008).
[27] H. Heiselberg, C. J. Pethick, H. Smith, and L. Viverit, Phys. Rev. Lett. **85**, 2418 (2000).
[28] Z. Wu and G. M. Bruun, Phys. Rev. Lett. **117**, 245302 (2016).
[29] J. M. Midtgaard, Z. Wu, and G. M. Bruun, Phys. Rev. A **96**, 033605 (2017).
[30] H. Shimahara, J. Phys. Soc. Jpn. **67**, 736 (1998).
[31] C. Mora and R. Combescot, Europhys. Lett. **66**, 833 (2004).
[32] Z. Wu, J. K. Block, and G. M. Bruun, Sci. Rep. **6**, 19038 (2016).
[33] E. H. Lieb, R. Seiringer, and J. Yngvason, Phys. Rev. B **66**, 134529 (2002).
[34] A. J. Leggett, Rev. Mod. Phys. **47**, 331 (1975).
[35] L. Landau, E. Lifshitz, and L. Pitaevskij, *Statistical Physics, Part 2: Theory of Condensed State*, Landau and Lifshitz Course of Theoretical Physics Vol. 9 (Butterworth-Heinemann, Oxford, 1980).